PHYSICAL REVIEW LETTERS

Exact Quantum Dynamics of a Bosonic Josephson Junction

Kaspar Sakmann, Alexej I. Streltsov, Ofir E. Alon, and Lorenz S. Cederbaum

Theoretische Chemie, Physikalisch-Chemisches Institut, Universität Heidelberg,
Im Neuenheimer Feld 229, D-69120 Heidelberg, Germany

The quantum dynamics of a one-dimensional bosonic Josephson junction is studied by solving the time-dependent many-boson Schrödinger equation numerically exactly. Already for weak interparticle interactions and on short time scales, the commonly employed mean-field and many-body methods are found to deviate substantially from the exact dynamics. The system exhibits rich many-body dynamics such as enhanced tunneling and a novel equilibration phenomenon of the junction depending on the interaction, which is attributed to a quick loss of coherence.

Recent experiments on interacting Bose-Einstein condensates in double-well traps have led to some of the most exciting results in quantum physics, including matter-wave interferometry [1,2], squeezing and entanglement [3,4], as well as work on high-precision sensors [5]. Particular attention has been paid to tunneling phenomena of interacting Bose-Einstein condensates in double wells, which in this context are referred to as bosonic Josephson junctions. Explicitly, Josephson oscillations and self-trapping (suppression of tunneling) with Bose-Einstein condensates have been predicted [6,7] and recently realized in experiments [8,9], drawing intensive interest [10–15].

For the first time in literature, we provide the numerically exact many-body quantum dynamics of a one-dimensional (1D) bosonic Josephson junction in this work. This is made possible by a breakthrough in the solution of the time-dependent many-boson Schrödinger equation. We use the exact solution to check the current understanding of bosonic Josephson junctions—commonly described by the popular Gross-Pitaevskii (GP) mean-field theory and the Bose-Hubbard (BH) many-body model—and to find novel phenomena. The results of the GP and BH theories are found to deviate substantially from the full many-body solution already for weak interactions and on short time scales. In particular, the well-known self-trapping effect is greatly reduced. We attribute these findings to a quick loss of the junction's coherence not captured by the common methods. For stronger interactions and on longer time scales, we find a novel equilibration dynamics in which the density and other observables of the junction tend towards stationary values. We show that the dynamics of bosonic Josephson junctions is much richer than what is currently known.

To compute the time evolution of the system, we solve the time-dependent many-boson Schrödinger equation by using the multiconfigurational time-dependent Hartree for bosons (MCTDHB) method [16]. In the MCTDHB(M) method, the time-dependent many-boson wave function is expanded in all time-dependent permanents $|\vec{n}; t\rangle$, generated by distributing N bosons over M time-dependent

orbitals $\{\phi_i(x, t)\}$. $\vec{n} = (n_1, n_2, \ldots, n_M)$ collects the occupation numbers. The MCTDHB wave function thus reads $|\Psi(t)\rangle = \sum_{\vec{n}} C_{\vec{n}}(t)|\vec{n}; t\rangle$. The expansion coefficients $\{C_{\vec{n}}(t)\}$ and orbitals $\{\phi_i(x, t)\}$ are determined by the Dirac-Frenkel time-dependent variational principle [16]. Our results are obtained by using a novel mapping of the many-boson configuration space in combination with a parallel implementation of MCTDHB, allowing the efficient handling of millions of time-dependent optimized permanents [17].

Having computed the many-boson wave function $|\Psi(t)\rangle$, we focus on the evolution of the following quantities to analyze the dynamics of the Josephson junction. The reduced one-body density matrix of the system is defined by $\rho^{(1)}(x|x'; t) = \langle\Psi(t)|\hat{\Psi}^\dagger(x')\hat{\Psi}(x)|\Psi(t)\rangle$, where $\hat{\Psi}(x)$ is the usual bosonic field operator annihilating a particle at position x. Its diagonal part, $\rho(x, t) \equiv \rho^{(1)}(x|x' = x; t)$, is simply the density of the system. As is common in the analysis of bosonic Josephson junctions, the "survival probability" of the system in, e.g., the left well, is obtained by integrating the density over the left well, $p_L(t) \equiv \frac{1}{N} \int_{-\infty}^{0} \rho(x, t)dx$. Furthermore, the eigenvalues $n_i^{(1)}$ of $\rho^{(1)}(x|x'; t)$ determine the extent to which the system is condensed or fragmented [18,19]. Finally, the first-order correlation function $g^{(1)}(x', x; t) \equiv \rho^{(1)}(x|x'; t)/\sqrt{\rho(x, t)\rho(x', t)}$ quantifies the system's degree of spatial coherence [20,21].

We now turn to the details of the 1D bosonic Josephson junction considered in this work. It is convenient to use dimensionless units defined by dividing the Hamiltonian by $\frac{\hbar^2}{mL^2}$, where m is the mass of a boson and L is a length scale. Realistic experimental parameters for the cases considered below are given in Ref. [22]. The full many-body Hamiltonian then reads $H = \sum_{i=1}^{N} h(x_i) + \sum_{i<j} W(x_i - x_j)$, where $h(x) = -\frac{1}{2}\frac{\partial^2}{\partial x^2} + V(x)$, with a trapping potential $V(x)$ and an interparticle interaction potential $W(x - x') = \lambda_0\delta(x - x')$. λ_0 is determined by the scattering length a_s and the transverse confinement $\omega_\perp$ [23]. In the following we assume repulsive interaction, $\lambda_0 > 0$. The symmetric double-well potential $V(x)$ is generated by connecting two harmonic potentials $V_\pm(x) = \frac{1}{2}(x \pm 2)^2$ with a

cubic spline in the region $|x| \leq 0.5$. The lowest four single-particle energy levels $e_1 = 0.473$, $e_2 = 0.518$, $e_3 = 1.352$, and $e_4 = 1.611$ of $V(x)$ are lower than the barrier height $V(0) = 1.667$.

Left- and right-localized orbitals $\phi_{L,R}$ can be constructed from the single-particle ground state and the first excited state of $V(x)$. ϕ_L and ϕ_R determine the parameters $U = \lambda_0 \int |\phi_L|^4$, $J = -\int \phi_L^* h \phi_R$, the Rabi oscillation period $t_{\mathrm{Rabi}} = \pi/J$, and the often employed interaction parameters, $\Lambda = UN/(2J)$ and U/J [6,7]. In this work, we use the interaction parameter $\lambda = \lambda_0(N-1)$, which appears naturally in the full many-body treatment, and quote the corresponding values for Λ and U/J. Within the framework of two-mode GP theory, a state, which is initially localized in one well, is predicted to remain self-trapped if $\Lambda > \Lambda_c = 2$ [6,7]. We will consider interaction strengths below, in the vicinity of, and above Λ_c.

In all of our computations, the system is prepared at $t = 0$ as the many-body ground state of the potential $V_+(x)$ and then propagated in the potential $V(x)$. Within the BH framework, this procedure amounts to starting from the state in which all bosons occupy the orbital ϕ_L.

We begin our studies with a weak interaction strength $\lambda = 0.152$, leading to $U/J = 0.140$ (0.027) and $\Lambda = 1.40$ (1.35) for $N = 20$ (100) bosons, which is well below the transition point for self-trapping $\Lambda_c = 2$. In the upper two panels of Fig. 1, the full many-body results for $p_L(t)$ are shown together with those of GP and BH theory. The full many-body dynamics is governed by three different time scales. On a time scale of the order of a Rabi cycle, $p_L(t)$ performs large-amplitude oscillations about $p_L = 0.5$, the long-time average of $p_L(t)$. The amplitude of these oscillations is damped out on a time scale of a few Rabi cycles and marks the beginning of a collapse and revival (not shown) sequence [6], which is also found on the full many-body level. On top of these slow large-amplitude oscillations, a higher frequency with a small amplitude can be seen. In a single-particle picture, these high frequency oscillations can be related to contributions from higher excited states in the initial wave function. However, a single-particle picture fails to describe the dynamics, as we shall now show. While the initial wave function $|\Psi(t = 0)\rangle$ is practically condensed—the fragmentation of the system is less than 10^{-4} (10^{-5}) for $N = 20$ (100) bosons—the propagated wave function $|\Psi(t)\rangle$ quickly becomes fragmented. The fragmentation increases to about 33% (26%) at $t = 3t_{\mathrm{Rabi}}$ for $N = 20$ (100) particles, making a many-body treatment indispensable already at this weak interaction strength. The respective GP results oscillate back and forth at a frequency close to the Rabi frequency and resemble the full many-body dynamics only on a time scale shorter than half a Rabi cycle. The poor quality of the GP mean-field approximation is, of course, due to the fact that the exact wave function starts to fragment while the GP dynamics remains condensed by construction.
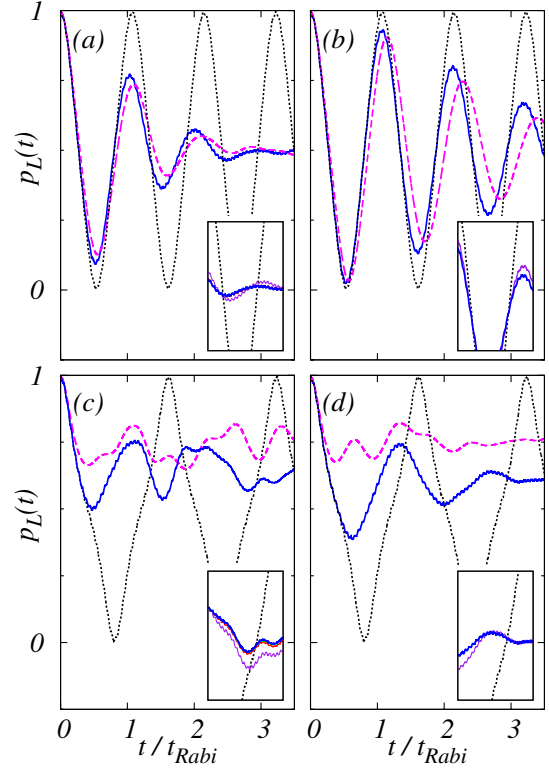

FIG. 1 (color online).   Full quantum dynamics of a 1D bosonic Josephson junction below ($\Lambda < \Lambda_c$) and above ($\Lambda > \Lambda_c$) the transition to self-trapping as defined by the two-mode GP theory. Shown is the full many-body result [solid (blue) lines] for the probability of finding a boson in the left well, $p_L(t)$. For comparison, the respective GP [dotted (black) lines] and BH [dashed (magenta) lines] results are shown as well. The parameter values are (a) $N = 20$, $\lambda = 0.152$, (b) $N = 100$, $\lambda = 0.152$ ($\Lambda < \Lambda_c$), (c) $N = 20$, $\lambda = 0.245$, and (d) $N = 100$, $\lambda = 0.245$ ($\Lambda > \Lambda_c$). The GP and BH results are found to deviate from the full many-body results already after short times. The insets show the convergence of the full many-body results. In the color online: (a), (c) $M = 2$ (solid purple line), $M = 4$ (solid red line), $M = 6$ (solid green line), and $M = 8$ (solid blue line). The $M = 2$ results are seen to deviate slightly from the converged results for $M \geq 4$. (b), (d) The results for $M = 2$ (solid purple line) and $M = 4$ (solid blue line) are shown. All quantities shown are dimensionless.

The BH result for $p_L(t)$ reproduces many features of the exact solution at this interaction strength for both $N = 20$ and $N = 100$ particles. The large-amplitude oscillations collapse over a period of a few Rabi cycles and revive at a later stage (not shown). Also, the BH solution quickly becomes fragmented, starting from the left localized state, which is totally condensed. The fragmentation of the BH wave function for $N = 20$ (100) particles at $t = 3t_{\mathrm{Rabi}}$ is essentially the same as the respective value of the exact solution. However, differences between the exact and the BH result are visible even on time scales less than half a Rabi cycle. Not only are the amplitudes obviously different, but the frequencies contained in $p_L(t)$ are different as well. Furthermore, the BH solutions do not exhibit a high

frequency oscillation on top of the slow large-amplitude oscillations, a difference which is related to the fact that the BH orbitals are time independent and thus not determined variationally at each point in time. Note that $p_L(t)$ is a quantity in which all spatial degrees of freedom have been integrated out. Visible differences in $p_L(t)$ imply that it is not only the densities $\rho(x, t)$ which must differ, but also all correlation functions.

The insets of Figs. 1(a) and 1(b) demonstrate the convergence of the many-body dynamics results. In particular and somewhat unexpectedly, the number of time-dependent orbitals needed to describe the bosonic Josephson junction dynamics quantitatively is $M = 4$, even below the transition point for self-trapping. These orbitals are determined variationally at each point in time, implying that any method using time-independent orbitals will need substantially more orbitals to achieve the same accuracy.

One of the central phenomena often discussed in the context of bosonic Josephson junctions is the celebrated self-trapping transition [6–9]. In what follows, we study the dynamics of a bosonic Josephson junction in the self-trapping regime from the full many-body perspective.

The interaction strength is taken to be $\lambda = 0.245$, leading to $U/J = 0.226$ (0.043) and $\Lambda = 2.26$ (2.17) for $N = 20$ (100) particles. Hence, the system is just above the critical value for self-trapping $\Lambda_c = 2$ [6,7]. The results for $N = 20$ and $N = 100$ are collected in Figs. 1(c) and 1(d). The exact solutions exhibit indeed some self-trapping on the time scale shown. The fragmentation of the condensate for $N = 20$ (100) bosons increases from initially less than 10^{-4} (10^{-5}) to about 28% (18%) after three Rabi cycles. Note that the system is now less fragmented than for weaker interactions after the same period of time. Nevertheless, GP theory is—as before—inapplicable, even on time scales shorter than $t_{\text{Rabi}}/2$. The BH results deviate from the true dynamics even earlier. They greatly overestimate the self-trapping and coherence of the condensate. According to the BH model, the condensate would only be 13% (11%) fragmented for $N = 20$ (100) at $t = 3t_{\text{Rabi}}$, which is not the case. This trend also continues for stronger interactions (see below). The following general statement about the relationship between self-trapping and coherence can be inferred from the exact results: self-trapping is only present as long as the system remains coherent. We find this statement to be true at all interaction strengths and all particle numbers considered in this work.

Let us briefly discuss the applicability of GP theory and the BH model to the cases considered above. 1D Bose gases are considered weakly interacting when the parameter $\sqrt{\gamma} = \sqrt{\lambda_0/\rho}$ [24] is small compared to one (ρ is a characteristic density). Using the peak density for ρ, we find $\frac{1}{200} < \sqrt{\gamma} < \frac{1}{30}$, showing that the above cases are weakly interacting. The BH model is expected to be valid when the chemical potential μ is well below the band gap $e_{\text{gap}} = e_3 - e_2$ and the initial state lies within the first band [6]. These conditions are well satisfied. We find $\mu/e_{\text{gap}} \approx$

$\frac{1}{14}$ and $\frac{1}{9}$ for the cases shown in Figs. 1(a) and 1(b) and Figs. 1(c) and 1(d), respectively. The overlap integral of the initial states' first natural orbital with the left BH orbital is 0.9991(!) in all cases; the initial states are therefore essentially given by the BH state $|N, 0\rangle$. The results do not depend significantly on this tiny difference. Clearly, we have shown a failure of GP theory and the BH model within their range of expected validity.

We now turn to the case of stronger interactions, $\lambda = 4.9$, which is well above the self-trapping transition point. This leads to $U/J = 9.55$ (0.869) and $\Lambda = 47.8$ (43.4) for $N = 10$ (100) bosons. Note that we now use 10 instead of 20 bosons to demonstrate convergence. The energy per particle of the full many-body wave function is now $E/N = 1.22$ (1.28) for $N = 10$ (100) bosons, which is still below the barrier height $V(0) = 1.667$. Although here we are outside of the range of expected validity of GP and BH, it is interesting to see what they fail to describe. Figure 2 (top) shows the full many-body results for $N = 10$ and $N = 100$ bosons together with those of the BH model. The two BH results lie on top of each other. In complete contrast to the BH dynamics, for which $p_L(t)$ remains trapped in the left well, the full many-body dynamics shows no self-trapping. Instead, a very intricate dynamics results, leading to an equilibration phenomenon in which the density of the system tends to be equally distributed over both wells.
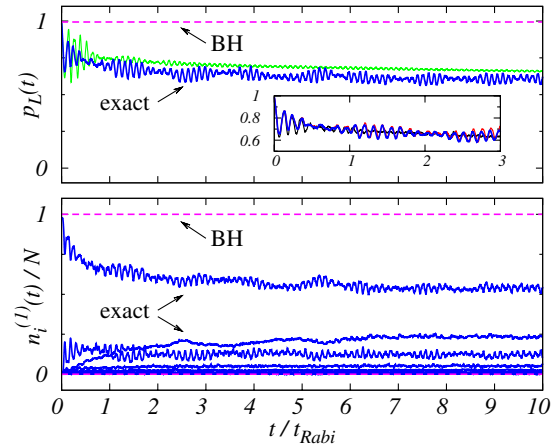

FIG. 2 (color online). Emergence of equilibration of the density at interaction strength $\lambda = 4.9$. Top: same as Fig. 1, but for $N = 10$ [solid black (blue) line] and $N = 100$ [solid gray (green) line]. The respective BH [dashed (magenta) line] results are on top of each other. In contrast to the BH dynamics, which is completely self-trapped, the full many-body dynamics is not. $p_L(t)$ tends towards its long-time average $p_L = 0.5$. For $N = 100$ particles, $M = 4$ orbitals were used. The inset shows the convergence of the full many-body solution for $N = 10$ bosons. In the color online: $M = 4$ (solid black line), $M = 10$ (solid blue line), and $M = 12$ (solid red line). The $M = 4$ result follows the trend of the converged $M = 12$ result. Bottom: corresponding natural-orbital occupations for $N = 10$ bosons. The system becomes fragmented and roughly four natural orbitals are macroscopically occupied. All quantities are dimensionless.
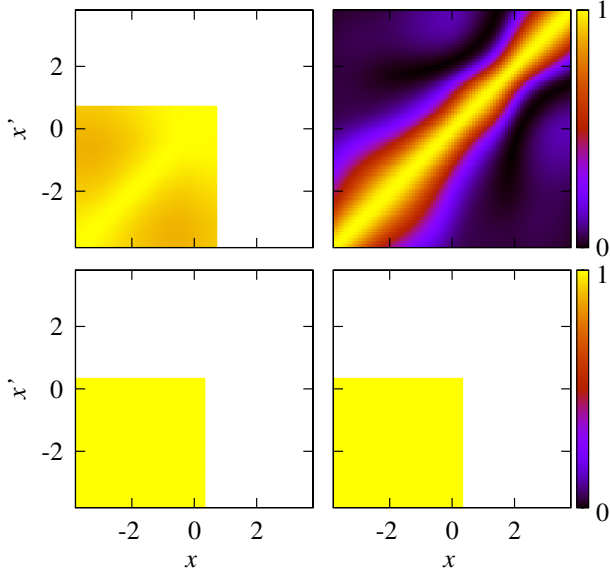
FIG. 3 (color online). Dynamics of the first-order correlation function for $\lambda = 4.9$ at which the equilibration phenomenon of Fig. 2 occurs. Shown is $|g^{(1)}(x', x; t)|^2$ of $N = 10$ bosons at different times. Top left: full many-body result at $t = 0$. The initial state exhibits coherence over the entire extent of the system. Top right: full many-body result at $t = 10 t_{\text{Rabi}}$. The coherence is lost. The system is incoherent even on short length scales. Bottom left: BH result at $t = 0$. Bottom right: BH result at $t = 10 t_{\text{Rabi}}$. In contrast to the full many-body result, the BH wave function remains completely coherent.

The system's full many-body dynamics is again strongly fragmented as can be seen in Fig. 2 (bottom), which depicts the natural-orbital occupations $n_i^{(1)}$ for $N = 10$ particles. This rules out any description of the system by GP theory which always predicts condensation. Also shown are the natural-orbital occupations of the BH model, which wrongly describes a fully condensed system although, in principle, this model can describe fragmentation.

The strong fragmentation of the system implies the presence of strong correlations. This can be seen in the two upper panels of Fig. 3, which show the full many-body result for the first-order correlation function $g^{(1)}(x', x; t)$ of $N = 10$ bosons at times $t = 0$ and $t = 10 t_{\text{Rabi}}$. The fragmentation of the initial state is only $\approx 2\%$, leading to an almost flat $g^{(1)}(x', x; 0)$. This reflects the fact that the system is initially coherent over its entire extent. At $t = 10 t_{\text{Rabi}}$, the coherence of the system is completely lost even on length scales much shorter than its size (see upper right panel of Fig. 3). Note that $g^{(1)}(x', x; t)$ also tends to equilibrate. The respective BH results for $g^{(1)}(x', x; t)$ are shown in the two lower panels of Fig. 3 and in contrast display no visible loss of coherence.

Let us briefly summarize. We have obtained exact results for the full many-body dynamics of a 1D bosonic Josephson junction. The dynamics is found to be much richer than previously reported. In particular, the predictions of the commonly employed Gross-Pitaevskii and Bose-Hubbard theories are found to differ substantially from the exact results already after short times and relatively weak interactions. These differences are associated with the development of fragmentation and correlations not captured by the standard theories. For stronger interactions, where the standard theories predict coherence and self-trapping, we find a completely different dynamics. The system becomes fragmented, spatial coherence is lost, and a long-time equilibration of the junction emerges. We hope our results stimulate experiments.

[1] M. R. Andrews *et al.*, Science **275**, 637 (1997).
[2] T. Schumm *et al.*, Nature Phys. **1**, 57 (2005).
[3] G.-B. Jo *et al.*, Phys. Rev. Lett. **98**, 030407 (2007).
[4] J. Estève *et al.*, Nature (London) **455**, 1216 (2008).
[5] B. V. Hall *et al.*, Phys. Rev. Lett. **98**, 030402 (2007).
[6] G. J. Milburn *et al.*, Phys. Rev. A **55**, 4318 (1997).
[7] A. Smerzi *et al.*, Phys. Rev. Lett. **79**, 4950 (1997).
[8] M. Albiez *et al.*, Phys. Rev. Lett. **95**, 010402 (2005).
[9] S. Levy *et al.*, Nature (London) **449**, 579 (2007).
[10] S. Raghavan *et al.*, Phys. Rev. A **59**, 620 (1999).
[11] C. Lee, Phys. Rev. Lett. **97**, 150402 (2006).
[12] D. Ananikian and T. Bergeman, Phys. Rev. A **73**, 013604 (2006).
[13] R. Gati and M. K. Oberthaler, J. Phys. B **40**, R61 (2007).
[14] G. Ferrini, A. Minguzzi, and F. W. J. Hekking, Phys. Rev. A **78**, 023606 (2008).
[15] X. Y. Jia, W. D. Li, and J. Q. Liang, Phys. Rev. A **78**, 023613 (2008).
[16] A. I. Streltsov, O. E. Alon, and L. S. Cederbaum, Phys. Rev. Lett. **99**, 030402 (2007); O. E. Alon, A. I. Streltsov, and L. S. Cederbaum, Phys. Rev. A **77**, 033613 (2008).
[17] A. I. Streltsov *et al.*, arXiv:0910.2577v1.
[18] A. I. Streltsov, O. E. Alon, and L. S. Cederbaum, Phys. Rev. A **73**, 063626 (2006).
[19] E. J. Mueller *et al.*, Phys. Rev. A **74**, 033612 (2006).
[20] M. Naraschewski and R. J. Glauber, Phys. Rev. A **59**, 4595 (1999).
[21] K. Sakmann *et al.*, Phys. Rev. A **78**, 023615 (2008).
[22] As an example, we choose $L = 1\ \mu$m and ^{87}Rb as a boson. Note that other realistic choices can be made. The unit of energy $\frac{\hbar^2}{mL^2}$ then corresponds to 116 Hz and the potential $V(x)$ has the following characteristics: barrier height $V(0)$: 193.9 Hz, distance between the minima: 4 μm, width (FWHM): 1.418 μm, and $t_{\text{Rabi}} =$ 192.4 msec. To realize the cases considered in this work, a_s and $\omega_\perp$ can be chosen as follows. For $\lambda = 0.152$, $N = 20$ (100): $a_s = 1.28$ (0.246) nm, $\frac{\omega_\perp}{2\pi} = 363.4$ Hz. For $\lambda = 0.245$, $N = 20$ (100): $a_s = 2.06$ (0.396) nm, $\frac{\omega_\perp}{2\pi} = 363.4$ Hz. For $\lambda = 4.9$, $N = 10$ (100): $a_s = 5.31$ nm, $\frac{\omega_\perp}{2\pi} = 5962$ (542.0) Hz.
[23] M. Olshanii, Phys. Rev. Lett. **81**, 938 (1998).
[24] E. H. Lieb and W. Liniger, Phys. Rev. **130**, 1605 (1963); D. S. Petrov, G. V. Shlyapnikov, and J. T. M. Walraven, Phys. Rev. Lett. **85**, 3745 (2000).